Evidence for the Direct Two-Photon Transition from $\psi(3686)$ to J/ψ

M. Ablikim,[1] M. N. Achasov,[5] D. J. Ambrose,[40] F. F. An,[1] Q. An,[41] Z. H. An,[1] J. Z. Bai,[1] R. B. Ferroli,[18] Y. Ban,[27] J. Becker,[2] N. Berger,[1] M. B. Bertani,[18] J. M. Bian,[39] E. Boger,[20,*] O. Bondarenko,[21] I. Boyko,[20] R. A. Briere,[3] V. Bytev,[20] X. Cai,[1] A. C. Calcaterra,[18] G. F. Cao,[1] J. F. Chang,[1] G. Chelkov,[20,*] G. Chen,[1] H. S. Chen,[1] J. C. Chen,[1] M. L. Chen,[1] S. J. Chen,[25] Y. Chen,[1] Y. B. Chen,[1] H. P. Cheng,[14] Y. P. Chu,[1] D. Cronin-Hennessy,[39] H. L. Dai,[1] J. P. Dai,[1] D. Dedovich,[20] Z. Y. Deng,[1] A. Denig,[19] I. Denysenko,[20,†] M. Destefanis,[44] W. M. Ding,[29] Y. Ding,[23] L. Y. Dong,[1] M. Y. Dong,[1] S. X. Du,[47] J. Fang,[1] S. S. Fang,[1] L. Fava,[44,‡] F. Feldbauer,[2] C. Q. Feng,[41] C. D. Fu,[1] J. L. Fu,[25] Y. Gao,[36] C. Geng,[41] K. Goetzen,[7] W. X. Gong,[1] W. Gradl,[19] M. Greco,[44] M. H. Gu,[1] Y. T. Gu,[9] Y. H. Guan,[6] A. Q. Guo,[26] L. B. Guo,[24] Y. P. Guo,[26] Y. L. Han,[1] X. Q. Hao,[1] F. A. Harris,[38] K. L. He,[1] M. He,[1] Z. Y. He,[26] T. Held,[2] Y. K. Heng,[1] Z. L. Hou,[1] H. M. Hu,[1] J. F. Hu,[6] T. Hu,[1] B. Huang,[1] G. M. Huang,[15] J. S. Huang,[12] X. T. Huang,[29] Y. P. Huang,[1] T. Hussain,[43] C. S. Ji,[41] Q. Ji,[1] X. B. Ji,[1] X. L. Ji,[1] L. K. Jia,[1] L. L. Jiang,[1] X. S. Jiang,[1] J. B. Jiao,[29] Z. Jiao,[14] D. P. Jin,[1] S. Jin,[1] F. F. Jing,[36] N. Kalantar-Nayestanaki,[21] M. Kavatsyuk,[21] W. Kuehn,[37] W. Lai,[1] J. S. Lange,[37] J. K. C. Leung,[35] C. H. Li,[1] Cheng Li,[41] Cui Li,[41] D. M. Li,[47] F. Li,[1] G. Li,[1] H. B. Li,[1] J. C. Li,[1] K. Li,[10] Lei Li,[1] N. B. Li,[24] Q. J. Li,[1] S. L. Li,[1] W. D. Li,[1] W. G. Li,[1] X. L. Li,[29] X. N. Li,[1] X. Q. Li,[26] X. R. Li,[28] Z. B. Li,[33] H. Liang,[41] Y. F. Liang,[31] Y. T. Liang,[37] G. R. Liao,[36] X. T. Liao,[1] B. J. Liu,[1] B. J. Liu,[34] C. L. Liu,[3] C. X. Liu,[1] C. Y. Liu,[1] F. H. Liu,[30] Fang Liu,[1] Feng Liu,[15] H. Liu,[1] H. B. Liu,[6] H. H. Liu,[13] H. M. Liu,[1] H. W. Liu,[1] J. P. Liu,[45] Kun Liu,[27] Kai Liu,[6] K. Y. Liu,[23] P. L. Liu,[29] S. B. Liu,[41] X. Liu,[22] X. H. Liu,[1] Y. B. Liu,[26] Y. Liu,[1] Z. A. Liu,[1] Zhiqiang Liu,[1] Zhiqing Liu,[1] H. Loehner,[21] G. R. Lu,[12] H. J. Lu,[14] J. G. Lu,[1] Q. W. Lu,[30] X. R. Lu,[6] Y. P. Lu,[1] C. L. Luo,[24] M. X. Luo,[46] T. Luo,[38] X. L. Luo,[1] M. Lv,[1] C. L. Ma,[6] F. C. Ma,[23] H. L. Ma,[1] Q. M. Ma,[1] S. Ma,[1] T. Ma,[1] X. Y. Ma,[1] Y. Ma,[11] F. E. Maas,[11] M. Maggiora,[44] Q. A. Malik,[43] H. Mao,[1] Y. J. Mao,[27] Z. P. Mao,[1] J. G. Messchendorp,[21] J. Min,[1] T. J. Min,[1] R. E. Mitchell,[17] X. H. Mo,[1] C. Morales Morales,[11] C. Motzko,[2] N. Yu. Muchnoi,[5] Y. Nefedov,[20] C. Nicholson,[6] I. B. Nikolaev,[5] Z. Ning,[1] S. L. Olsen,[28] Q. Ouyang,[1] S. P. Pacetti,[18,§] J. W. Park,[28] M. Pelizaeus,[38] K. Peters,[7] J. L. Ping,[24] R. G. Ping,[1] R. Poling,[39] E. Prencipe,[19] C. S. J. Pun,[35] M. Qi,[25] S. Qian,[1] C. F. Qiao,[6] X. S. Qin,[1] Y. Qin,[27] Z. H. Qin,[1] J. F. Qiu,[1] K. H. Rashid,[43] G. Rong,[1] X. D. Ruan,[9] A. Sarantsev,[20,∥] J. Schulze,[2] M. Shao,[41] C. P. Shen,[38,¶] X. Y. Shen,[1] H. Y. Sheng,[1] M. R. Shepherd,[17] X. Y. Song,[1] S. Spataro,[44] B. Spruck,[37] D. H. Sun,[1] G. X. Sun,[1] J. F. Sun,[12] S. S. Sun,[1] X. D. Sun,[1] Y. J. Sun,[41] Y. Z. Sun,[1] Z. J. Sun,[1] Z. T. Sun,[41] C. J. Tang,[31] X. Tang,[1] E. H. Thorndike,[40] H. L. Tian,[1] D. Toth,[39] M. U. Ulrich,[37] G. S. Varner,[38] B. Wang,[9] B. Q. Wang,[27] K. Wang,[1] L. L. Wang,[4] L. S. Wang,[1] M. Wang,[29] P. Wang,[1] P. L. Wang,[1] Q. Wang,[1] Q. J. Wang,[1] S. G. Wang,[27] X. F. Wang,[12] X. L. Wang,[41] Y. D. Wang,[41] Y. F. Wang,[1] Y. Q. Wang,[29] Z. Wang,[1] Z. G. Wang,[1] Z. Y. Wang,[1] D. H. Wei,[8] P. Weidenkaff,[19] Q. G. Wen,[41] S. P. Wen,[1] M. W. Werner,[37] U. Wiedner,[2] L. H. Wu,[1] N. Wu,[1] S. X. Wu,[41] W. Wu,[26] Z. Wu,[1] L. G. Xia,[36] Z. J. Xiao,[24] Y. G. Xie,[1] Q. L. Xiu,[1] G. F. Xu,[1] G. M. Xu,[27] H. Xu,[1] Q. J. Xu,[10] X. P. Xu,[32] Y. Xu,[26] Z. R. Xu,[41] F. Xue,[15] Z. Xue,[1] L. Yan,[41] W. B. Yan,[41] Y. H. Yan,[16] H. X. Yang,[1] T. Yang,[9] Y. Yang,[15] Y. X. Yang,[8] H. Ye,[1] M. Ye,[1] M. H. Ye,[4] B. X. Yu,[1] C. X. Yu,[26] J. S. Yu,[22] S. P. Yu,[29] C. Z. Yuan,[1] W. L. Yuan,[24] Y. Yuan,[1] A. A. Zafar,[43] A. Z. Zallo,[18] Y. Zeng,[16] B. X. Zhang,[1] B. Y. Zhang,[1] C. C. Zhang,[1] D. H. Zhang,[1] H. H. Zhang,[33] H. Y. Zhang,[1] J. Zhang,[24] J. G. Zhang,[12] J. Q. Zhang,[1] J. W. Zhang,[1] J. Y. Zhang,[1] J. Z. Zhang,[1] L. Zhang,[25] S. H. Zhang,[1] T. R. Zhang,[24] X. J. Zhang,[1] X. Y. Zhang,[29] Y. Zhang,[1] Y. H. Zhang,[1] Y. S. Zhang,[9] Z. P. Zhang,[41] Z. Y. Zhang,[45] G. Zhao,[1] H. S. Zhao,[1] J. W. Zhao,[1] K. X. Zhao,[24] Lei Zhao,[41] Ling Zhao,[1] M. G. Zhao,[26] Q. Zhao,[1] S. J. Zhao,[47] T. C. Zhao,[1] X. H. Zhao,[25] Y. B. Zhao,[1] Z. G. Zhao,[41] A. Zhemchugov,[20,*] B. Zheng,[42] J. P. Zheng,[1] Y. H. Zheng,[6] Z. P. Zheng,[1] B. Zhong,[1] J. Zhong,[2] L. Zhou,[1] X. K. Zhou,[6] X. R. Zhou,[41] C. Zhu,[1] K. Zhu,[1] K. J. Zhu,[1] S. H. Zhu,[1] X. L. Zhu,[36] X. W. Zhu,[1] Y. M. Zhu,[26] Y. S. Zhu,[1] Z. A. Zhu,[1] J. Zhuang,[1] B. S. Zou,[1] J. H. Zou,[1] and J. X. Zuo[1]

(BESIII Collaboration)

[1]*Institute of High Energy Physics, Beijing 100049, People's Republic of China*
[2]*Bochum Ruhr-University, 44780 Bochum, Germany*
[3]*Carnegie Mellon University, Pittsburgh, Pennsylvania 15213, USA*
[4]*China Center of Advanced Science and Technology, Beijing 100190, People's Republic of China*
[5]*G. I. Budker Institute of Nuclear Physics SB RAS (BINP), Novosibirsk 630090, Russia*
[6]*Graduate University of Chinese Academy of Sciences, Beijing 100049, People's Republic of China*
[7]*GSI Helmholtzcentre for Heavy Ion Research GmbH, D-64291 Darmstadt, Germany*
[8]*Guangxi Normal University, Guilin 541004, People's Republic of China*
[9]*GuangXi University, Nanning 530004, People's Republic of China*

[10]Hangzhou Normal University, Hangzhou 310036, People's Republic of China

[11]Helmholtz Institute Mainz, J. J. Becherweg 45, D 55099 Mainz, Germany

[12]Henan Normal University, Xinxiang 453007, People's Republic of China

[13]Henan University of Science and Technology, Luoyang 471003, People's Republic of China

[14]Huangshan College, Huangshan 245000, People's Republic of China

[15]Huazhong Normal University, Wuhan 430079, People's Republic of China

[16]Hunan University, Changsha 410082, People's Republic of China

[17]Indiana University, Bloomington, Indiana 47405, USA

[18]INFN Laboratori Nazionali di Frascati, Frascati 00044, Italy

[19]Johannes Gutenberg University of Mainz, Johann-Joachim-Becher-Weg 45, 55099 Mainz, Germany

[20]Joint Institute for Nuclear Research, 141980 Dubna, Russia

[21]KVI/University of Groningen, 9747 AA Groningen, Netherlands

[22]Lanzhou University, Lanzhou 730000, People's Republic of China

[23]Liaoning University, Shenyang 110036, People's Republic of China

[24]Nanjing Normal University, Nanjing 210046, People's Republic of China

[25]Nanjing University, Nanjing 210093, People's Republic of China

[26]Nankai University, Tianjin 300071, People's Republic of China

[27]Peking University, Beijing 100871, People's Republic of China

[28]Seoul National University, Seoul, 151-747, Korea

[29]Shandong University, Jinan 250100, People's Republic of China

[30]Shanxi University, Taiyuan 030006, People's Republic of China

[31]Sichuan University, Chengdu 610064, People's Republic of China

[32]Soochow University, Suzhou 215006, People's Republic of China

[33]Sun Yat-Sen University, Guangzhou 510275, People's Republic of China

[34]The Chinese University of Hong Kong, Shatin, New Territories, Hong Kong

[35]The University of Hong Kong, Pokfulam, Hong Kong

[36]Tsinghua University, Beijing 100084, People's Republic of China

[37]Universitaet Giessen, 35392 Giessen, Germany

[38]University of Hawaii, Honolulu, Hawaii 96822, USA

[39]University of Minnesota, Minneapolis, Minnesota 55455, USA

[40]University of Rochester, Rochester, New York 14627, USA

[41]University of Science and Technology of China, Hefei 230026, People's Republic of China

[42]University of South China, Hengyang 421001, People's Republic of China

[43]University of the Punjab, Lahore 54590, Pakistan

[44]University of Turin and INFN, Turin 10125, Italy

[45]Wuhan University, Wuhan 430072, People's Republic of China

[46]Zhejiang University, Hangzhou 310027, People's Republic of China

[47]Zhengzhou University, Zhengzhou 450001, People's Republic of China

The two-photon transition $\psi(3686) \rightarrow \gamma\gamma J/\psi$ is studied in a sample of 1.06×10^8 $\psi(3686)$ decays collected by the BESIII detector. The branching fraction is measured to be $(3.1 \pm 0.6(\text{stat})^{+0.8}_{-1.0}(\text{syst})) \times 10^{-4}$ using $J/\psi \rightarrow e^+ e^-$ and $J/\psi \rightarrow \mu^+ \mu^-$ decays, and its upper limit is estimated to be 4.5×10^{-4} at the 90% confidence level. This work represents the first measurement of a two-photon transition among charmonium states. The orientation of the $\psi(3686)$ decay plane and the J/ψ polarization in this decay are also studied. In addition, the product branching fractions of sequential $E1$ transitions $\psi(3686) \rightarrow \gamma\chi_{cJ}$ and $\chi_{cJ} \rightarrow \gamma J/\psi (J = 0, 1, 2)$ are reported.

The XYZ [1] particles, which do not fit potential model expectations in QCD theory, have been a key challenge to the QCD description of charmoniumlike states [2]. To fully understand those states, it is necessary to consider the coupling of a charmonium state to a $D\bar{D}$ meson pair. These coupled-channel effects, which also play an important role in the charmonium transitions of low-lying states [i.e., from $\psi(3686)$ to J/ψ], are especially relevant for the radiative transition processes [3]. In the well-known electric dipole transitions, the strength of coupled-channel effects will likely be hard to establish, since the accompanying relativistic corrections may be more important [4]. However, the two-photon transition $\psi(3686) \rightarrow \gamma\gamma J/\psi$ is more sensitive to the coupled-channel effect and thus provides a unique opportunity to investigate these issues [5].

Two-photon spectroscopy has been a very powerful tool for the study of the excitation spectra of a variety of

systems with a wide range of sizes, such as molecules, atomic hydrogen, and positronium [6]. Studying the analogous process in quarkonium states is a natural extension of this work, in order to gain insight into nonperturbative QCD phenomena. But, so far, two-photon transitions in quarkonia have eluded experimental observation [7–9]. For example, in a study of $\psi(3686) \to \gamma \chi_{cJ}(J = 0, 1, 2)$ reported by the CLEO Collaboration [9], the upper limit for $\mathcal{B}(\psi(3686) \to \gamma\gamma J/\psi)$ was estimated to be 1×10^{-3}.

This Letter presents the first evidence for the two-photon transition $\psi(3686) \to \gamma\gamma J/\psi$, as well as studies of the orientation of the $\psi(3686)$ decay plane and the J/ψ polarization in the decay. The branching fractions of double $E1$ transitions $\psi(3686) \to \gamma(\gamma J/\psi)_{\chi_{cJ}}$ through χ_{cJ} intermediate states are also reported. The data analyzed were obtained by the BESIII experiment [10] viewing electron-positron collisions at the BEPCII collider. An integrated luminosity of 156.4 pb^{-1} was obtained at a center-of-mass energy $\sqrt{s} = M(\psi(3686)) = 3.686$ GeV. The number of $\psi(3686)$ decays in this sample is estimated to be $(1.06 \pm 0.04) \times 10^8$ [11]. In addition, 42.6 pb^{-1} of continuum data were taken below the $\psi(3686)$, at $\sqrt{s} = 3.65$ GeV, to evaluate the potential backgrounds from non-resonant events.

The upgraded BEPCII [12] at Beijing is a two-ring electron-positron collider. The BESIII detector [10] is an approximately cylindrically symmetric detector which covers 93% of the solid angle around the collision point. In the order of increasing distance from the interaction point, the subdetectors include a 43-layer main wire drift chamber (MDC), a time-of-flight system with two layers in the barrel region and one layer for each end cap, and a 6240 cell CsI(Tl) crystal electromagnetic calorimeter (EMC) with both barrel and end cap sections. The barrel components reside within a superconducting solenoid magnet providing a 1.0 T magnetic field aligned with the beam axis. Finally, there is a muon chamber consisting of nine layers of resistive plate chambers within the return yoke of the magnet. The momentum resolution for charged tracks in the MDC is 0.5% for transverse momenta of 1 GeV/c. The energy resolution for showers in the EMC is 2.5% for 1 GeV photons.

This work studies $\psi(3686) \to \gamma\gamma J/\psi$ followed by $J/\psi \to \ell^+\ell^-$ (ℓ denotes e or μ), which is referred to as the signal process. Events selected contain exactly two oppositely charged good tracks in the MDC tracking system, corresponding to the dilepton from J/ψ decay. The requirements to judge a track as good include $|\cos\theta| < 0.93$ (θ is the polar angle with respect to the beam direction) and the minimum distance of approach between the track and the production vertex less than 10 cm along the beam axis and less than 1 cm projected in the perpendicular plane. The lepton is identified with the ratio of EMC shower energy to MDC track momentum, E/p, which must be larger than 0.7 for an electron or smaller than 0.6

for a muon. To suppress non-J/ψ decay leptons, we require the momentum of each lepton to be larger than 0.8 GeV/c. A vertex fit (VF) constrains the production vertex, which is updated run-by-run, and the tracks of the dilepton candidates to a common vertex; only events with $\chi^2_{\mathrm{VF}}/\mathrm{d.o.f.} < 20$ are accepted.

Reconstructed EMC showers unmatched to either charged track and with an energy larger than 25 MeV in the barrel region ($|\cos\theta| < 0.80$) or larger than 50 MeV in the end caps ($0.86 < |\cos\theta| < 0.92$) are used as photon candidates. To reject bremsstrahlung photons, showers matching the initial momentum of either lepton within 10° are also discarded. Showers from noise, not originating from the beam collision, are suppressed by requiring the EMC cluster time to lie within a 700 ns window near the event start time.

Events are required to have only two photon candidates. A kinematic fit (KF) constrains the vertexed dilepton to the nominal mass of the intermediate J/ψ and the resulting J/ψ and photon candidates to the known initial four-momentum of the $\psi(3686)$. The KF fit quality χ^2_{KF} is required to be $\chi^2_{\mathrm{KF}}/\mathrm{d.o.f.} < 12$. For convenience, we use γ_{lg} (γ_{sm}) to denote the larger (smaller) energy photon. As indicated in Fig. 1(a), J/ψ candidates are identified with the requirement that the recoil mass of the two photons, $M_{\gamma\gamma\text{-recoil}}$, is within (3.08, 3.14) GeV/c^2.

Scatter plots of recoiling mass $M_{\gamma_{\mathrm{sm}}\text{-recoil}}$ from the lower energy photon γ_{sm} versus the invariant mass of two photons $M_{\gamma\gamma}$ are shown in Fig. 1, where clear resonance bands are seen from the decays $\psi(3686) \to \gamma\chi_{cJ}(J = 0, 1, 2)$ (three horizontal bands) and $\psi(3686) \to \pi^0(\eta)J/\psi$ (two vertical bands). As indicated in Fig. 1(c), the continuum
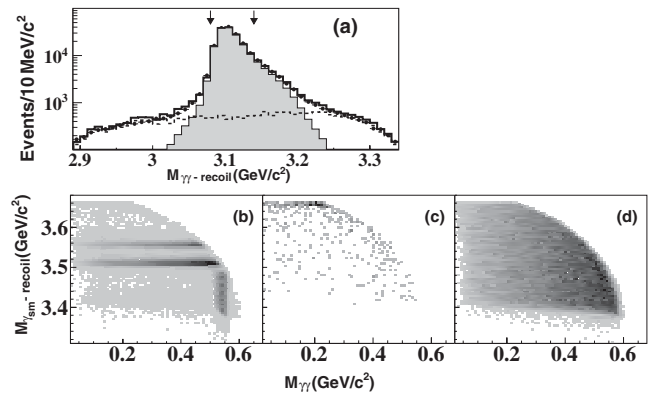

FIG. 1. Top: (a) distributions of $M_{\gamma\gamma\text{-recoil}}$ in data (points) and in the combined data set (solid line) of MC simulation of $\psi(3686)$ decays (shaded histogram) and continuum backgrounds (dashed line), before the KF is applied. The arrows indicate the window to select a J/ψ candidate. Bottom: scatter plots of $M_{\gamma_{\mathrm{sm}}\text{-recoil}}$ versus $M_{\gamma\gamma}$ for the $\gamma\gamma e^+e^-$ channel, in (b) data, (c) continuum data, and (d) MC simulated signal, after applying the KF constraint and the $M_{\gamma\gamma\text{-recoil}}$ window. The corresponding plots for the $\gamma\gamma\mu^+\mu^-$ channel are very similar.

backgrounds are most dominant at the tops of the plots, of which the primary sources include the Bhabha scattering, the dimuon process, and the initial-state radiation production of J/ψ. These backgrounds are excluded by discarding events with $M_{\gamma_{sm}\text{-recoil}} > 3.6$ GeV/c^2. To suppress backgrounds from $\psi(3686) \rightarrow \pi^0(\eta)J/\psi$, the diphoton invariant mass $M_{\gamma\gamma}$ is required to be larger than 0.15 GeV/c^2 and the recoil momentum of the diphoton must be larger than 0.25 GeV/c.

Monte Carlo (MC) simulations of $\psi(3686)$ decays are used to understand the backgrounds and also to estimate the detection efficiency. At BESIII, the simulation includes the beam energy spread and treats the initial-state radiation with KKMC [13]. Specific decay modes from the Particle Data Group (PDG) [14] are modeled with EVTGEN [15], and the unknown decay modes with Lundcharm [16]. The detector response is described using GEANT4 [17]. For the $\psi(3686) \rightarrow \gamma\gamma J/\psi$ channel, the momenta of decay particles are simulated according to the measured polarization structure in this work. Generic $\psi(3686)$ decay samples serve for understanding the background channels; dominant backgrounds were generated with high statistics. Angular distributions of the cascade $E1$ transitions $\psi(3686) \rightarrow \gamma\gamma\chi_{cJ} \rightarrow \gamma\gamma J/\psi$ are assumed to follow the formulas in Ref. [18]. Note that the χ_{cJ} line shapes were simulated with the Breit-Wigner distributions weighted with $E_{\gamma_1^*}^3 E_{\gamma_2^*}^3$ to account for the double $E1$ transitions and extended out to ±200 MeV/c^2 away from the nominal masses, using masses and widths in the PDG [14]. Here, $E_{\gamma_1^*}(E_{\gamma_2^*})$ is the energy of the radiative photon $\gamma_1^*(\gamma_2^*)$ in the rest frame of the mother particle $\psi(3686)(\chi_{cJ})$.

The yield of the signal process $\psi(3686) \rightarrow \gamma\gamma J/\psi$, together with those of the cascade $E1$ transition processes, is estimated by a global fit to the spectrum of $M_{\gamma_{sm}\text{-recoil}}$. The fit results are shown in Fig. 2. The shape and magnitude of $\psi(3686)$ decay backgrounds were fixed based on MC simulation. Non-$\psi(3686)$ decay backgrounds are estimated in continuum data, scaling by luminosity, and the $1/s$ dependence of the cross sections. This scaling is verified by the good description of the J/ψ backgrounds in the $M_{\gamma\gamma\text{-recoil}}$ distribution shown in Fig. 1(a). The
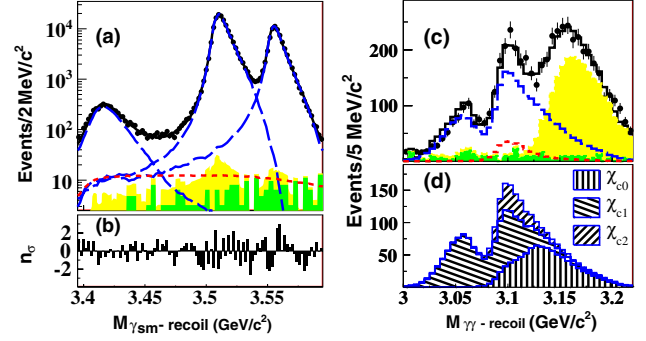

FIG. 2 (color online). (a) Unbinned maximum likelihood fit to the distribution of $M_{\gamma_{sm}\text{-recoil}}$ in data with combination of the two J/ψ decay modes. Thick lines are the sum of the fitting models, and long-dashed lines are the χ_{cJ} shapes. Short-dashed lines represent the two-photon signal processes. The light shaded histogram is $\psi(3686)$ decay backgrounds (yellow), and the dark shaded histogram is non-$\psi(3686)$ backgrounds (green), with the fixed amplitude and shape taken from MC simulation and continuum data. (b) The number of standard deviations, n_σ, of data points from the fitted curves in (a). The rates of the signal process and sequential χ_{cJ} processes are derived from these fits. (c) Distributions of $M_{\gamma\gamma\text{-recoil}}$ in data (signals and known backgrounds) with the kinematic requirement 3.44 GeV/$c^2 < M_{\gamma_{sm}\text{-recoil}} < 3.48$ GeV/c^2 and with the removal of χ_{KF}^2 and $M_{\gamma\gamma\text{-recoil}}$ restrictions. (d) Stacked histograms of the three χ_{cJ} components in (c).

distributions of the signal process and the cascade $E1$ process are taken from the reconstructed shapes in MC simulation of the modes and smeared with an asymmetric Gaussian with free parameters, which is used to compensate for the difference in line shape between MC simulations and data. By taking the MC shape, detector resolution and wrong assignment of the $E1$ photon are taken into account. The quality of goodness-of-fit test χ^2/d.o.f. = $108.0/94 = 1.15$ in the $\gamma\gamma e^+e^-$ mode and $124.8/94 = 1.33$ in the $\gamma\gamma\mu^+\mu^-$ mode. The observed signal yields are given in Table I. The $\psi(3686) \rightarrow \gamma\gamma J/\psi$ transition is observed with a statistical significance of 6.6σ, as determined by the ratio of the maximum likelihood value and the likelihood value for a fit with null-signal hypothesis. When the systematic uncertainties are taken into account

TABLE I. For different channels: the number of observed signals n_e (n_μ) and detection efficiency ϵ_e (ϵ_μ) in the $\gamma\gamma e^+e^-$ ($\gamma\gamma\mu^+\mu^-$) mode; the absolute branching fractions. On the bottom, the relative branching fractions $R_{MN} \equiv \mathcal{B}_{\chi_{cM}}/\mathcal{B}_{\chi_{cN}}$, where $\mathcal{B}_{\chi_{cJ}} \equiv \mathcal{B}(\psi(3686) \rightarrow \gamma(\gamma J/\psi)_{\chi_{cJ}})$ are listed. Here, the first errors are statistical and the second are systematic.

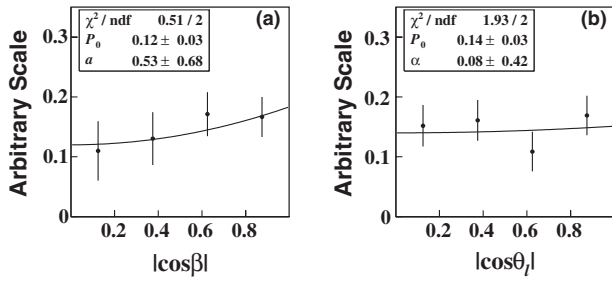| Channels	n_e	$\epsilon_e(\%)$	n_μ	$\epsilon_\mu(\%)$	$\mathcal{B}(\times10^{-4})$
$\gamma\gamma J/\psi$	564 ± 116	22.4	536 ± 128	30.0	$3.1 \pm 0.6^{+0.8}_{-1.0}$
$\gamma(\gamma J/\psi)_{\chi_{c0}}$	1801 ± 60	19.3	2491 ± 69	26.0	$15.1 \pm 0.3 \pm 1.0$
$\gamma(\gamma J/\psi)_{\chi_{c1}}$	$59\,953 \pm 253$	28.5	$81\,922 \pm 295$	38.2	$337.7 \pm 0.9 \pm 18.3$
$\gamma(\gamma J/\psi)_{\chi_{c2}}$	$32\,171 \pm 187$	27.5	$44\,136 \pm 219$	37.1	$187.4 \pm 0.7 \pm 10.2$
$R_{21} \equiv \frac{\mathcal{B}_{\chi_{c2}}}{\mathcal{B}_{\chi_{c1}}}(\%)$		$R_{01} \equiv \frac{\mathcal{B}_{\chi_{c0}}}{\mathcal{B}_{\chi_{c1}}}(\%)$		$R_{02} \equiv \frac{\mathcal{B}_{\chi_{c0}}}{\mathcal{B}_{\chi_{c2}}}(\%)$	
$55.47 \pm 0.26 \pm 0.11$		$4.45 \pm 0.09 \pm 0.18$		$8.03 \pm 0.17 \pm 0.33$	

FIG. 3.   (a) The corrected distribution of the normal angle β of the $\psi(3686)$ decay plane, and (b) the helicity angle θ_ℓ of J/ψ decays. The curves in (a) and (b) present the fits of functions $P_0(1 + a\cos^2\beta)$ and $P_0(1 + \alpha\cos^2\theta_\ell)$, respectively.

with the assumption of Gaussian distributions, the significance is evaluated to be 3.8σ, which corresponds to a probability of a background fluctuation to the observed signal yield of 7.2×10^{-5}. The upper limit for $\mathcal{B}(\psi(3686) \rightarrow \gamma\gamma J/\psi)$ is estimated to be 4.5×10^{-4} at the 90% confidence level, including systematic uncertainties.

In calculating $\mathcal{B}(\gamma\gamma J/\psi)$, a correction factor is included due to the interferences among χ_{cJ} states. This effect was checked by the variations of the observed signals in the global fit with inclusion of a floating interference component, which is modeled by the detector-smeared shape of a theoretical calculation [5]. It is found that relative changes on the signal yields are negative with lower bound of -10%. Hence, a correction factor 0.95 is assigned and 5% is taken as systematic uncertainty.

A cross-check on our procedures is performed with the $M_{\gamma\gamma\text{-recoil}}$ spectrum for the events in the region

$3.44 \text{ GeV}/c^2 < M_{\gamma_{\text{sm}}\text{-recoil}} < 3.48 \text{ GeV}/c^2$ without restrictions on χ^2_{KF} and $M_{\gamma\gamma\text{-recoil}}$, as shown in Fig. 2(c). An excess of data above known backgrounds can be seen around the J/ψ nominal mass, which is expected from the sought-after two-photon process. With the inclusion of the estimated yields of the signal process, the excess is well understood. The high-mass peak above the J/ψ peak comes from the backgrounds of $\psi(3686) \rightarrow \pi^0\pi^0 J/\psi$ decays. This satellite peak can be well described in MC simulation. In Fig. 2(d), the three χ_{cJ} tails show distinguishable distributions; the small left bump is from the χ_{c1} tail, while the χ_{c0} tail is dominant at the right side. The distribution in data in Fig. 2(c) can only be well described by the simulated χ_{cJ} shapes.

The angle of the normal axis of the $\psi(3686)$ decay plane with respect to the $\psi(3686)$ polarization vector (aligned to the beam axis), β, can be determined in our data. The event rate may be expressed, to leading order, as $\frac{dN}{d\cos\beta} \propto 1 + a\cos^2\beta$. The measurement was carried out in the rest frame of the $\psi(3686)$, and the decay plane of the $\psi(3686)$ was determined with the momenta of the two decay particles J/ψ and γ_{lg}. The signal yields in each angular bin were extracted by the global fit to the corresponding data set following the aforementioned procedure. After correction of the extracted signal yields with the detection efficiency, Fig. 3(a) shows the fit to the distribution of $|\cos\beta|$ for the sum of the two dilepton modes; we obtain $a = 0.53 \pm 0.68$.

The polarization of J/ψ should be helpful in understanding the mechanism of the transition process [19]. The polarization parameter α can be evaluated from the angular distribution of the decay rate, expressed as

TABLE II.   Summary of the systematic uncertainties on the measurement of $\mathcal{B}_{\text{sig}}$ of the $\gamma\gamma J/\psi$ signal process, $\mathcal{B}_{\chi_{cJ}}$ for χ_{cJ} intermediate processes, and the relative branching fractions R_{MN}, following the notation convention in Table I. The total systematic uncertainty is the square root of the sum. Centered dots ($\cdots$) mean that the uncertainty is negligible. Values inside the parentheses are for the $\gamma\gamma\mu^+\mu^-$ mode, while values outside are for the $\gamma\gamma e^+e^-$ mode. Numbers without brackets represent uncertainties that are common to both modes.

Systematic uncertainty (%)		$\mathcal{B}_{\text{sig}}$	$\mathcal{B}_{\chi_{c0}}$	$\mathcal{B}_{\chi_{c1}}$	$\mathcal{B}_{\chi_{c2}}$	R_{01}	R_{02}	R_{21}
Lepton track		2(2)	2(2)	2(2)	2(2)			
Photon shower		2	2	2	2			
Number of photons		10(3)	1(1)	1(1)	1(1)	2($\cdots$)	2($\cdots$)	$\cdots$($\cdots$)
KF, χ^2_{KF} requirement		2(2)	2(2)	2(2)	2(2)			
χ_{cJ} widths		$^{+15}_{-25}$	3	$\cdots$	$\cdots$	4	4	0.2
$M_{\gamma_{\text{sm}}\text{-recoil}}$ resolution		4(5)	$\cdots$($\cdots$)	$\cdots$($\cdots$)	$\cdots$($\cdots$)	$\cdots$($\cdots$)	$\cdots$($\cdots$)	$\cdots$($\cdots$)
Other background		4(2)	1(1)	$\cdots$($\cdots$)	$\cdots$($\cdots$)	$\cdots$($\cdots$)	$\cdots$($\cdots$)	$\cdots$($\cdots$)
χ_{cJ} interference		5	1	$\cdots$	$\cdots$	1	1	$\cdots$
Fitting		8(5)	1(1)	$\cdots$($\cdots$)	$\cdots$($\cdots$)	1(1)	1(1)	$\cdots$($\cdots$)
Spin structure		20	1	$\cdots$	$\cdots$	1	1	$\cdots$
Number of $\psi(3686)$		4	4	4	4			
$\mathcal{B}(J/\psi \rightarrow \ell^+\ell^-)$		1	1	1	1			
Total	Correlated	14(8)	3(3)	3(3)	3(3)	2(1)	2(1)	$\cdots$($\cdots$)
	Uncorrelated	$^{+25}_{-33}$	6	5	5	4	4	0.2

$\frac{dN}{d\cos\theta_\ell} \propto 1 + \alpha\cos^2\theta_\ell$. Here, $\alpha = \frac{\Gamma_T - 2\Gamma_L}{\Gamma_T + 2\Gamma_L}$ (with Γ_T and Γ_L being the transversely and longitudinally polarized decay widths, respectively) and the helicity angle θ_ℓ is defined as the angle of the lepton in the J/ψ rest frame with respect to the J/ψ boost direction in the laboratory frame. For fully transverse (longitudinal) polarization, $\alpha = +1(-1)$. Figure 3(b) shows the distribution of $|\cos\theta_\ell|$ for the sum of the two dilepton modes, after correcting the signal yields for the detection efficiency and the lepton final state radiation effect. Our fit result is $\alpha = 0.08 \pm 0.42$.

Sources of systematic errors on the measurement of branching fractions are listed in Table II. Uncertainties associated with the efficiency of the lepton tracking and identification were studied with a selected control sample of $\psi(3686) \to \pi^+\pi^-(\ell^+\ell^-)_{J/\psi}$. The potential bias due to limiting the maximum number of photon candidates was studied by varying the limit. Throughout the photon energy region in this work, the detection and energy resolution of the photons are well-modeled within a 1% uncertainty [11,20]. Detector resolution of the χ_{cJ} tails is taken into account up to the accuracy of the MC simulation. The corresponding systematic uncertainty is evaluated by scanning the sizes of smearing parameters within their errors. For the signal process, the dominant uncertainties are from the description of χ_{cJ} line shapes, e.g., χ_{cJ} widths. The sensitivity to the χ_{cJ} widths is studied by a comparison of the signal yields based on different settings of the χ_{cJ} widths in modeling the χ_{cJ} resonances within the current world-average uncertainties. Relative changes of the signal detection efficiencies are assigned as 20% by varying the input spin structure within the measurement uncertainties and weighting the efficiencies in the Dalitz-like plot of Fig. 1(d).

Many sources of systematic uncertainties in Table II cancel out when extracting the $\psi(3686)$ decay plane parameter a and the J/ψ polarization parameter α. The quadrature sums of the remaining systematic uncertainties are $^{+0.68}_{-0.27}$ and $^{+0.07}_{-0.14}$ for a and α, respectively.

To summarize, the first measurement of the two-photon transition $\psi(3686) \to \gamma\gamma J/\psi$ was carried out at the BESIII experiment. The branching fraction is given in Table I, as well as those of the cascade $E1$ transitions. The measurement of the two-photon process is consistent with the upper limit obtained in Ref. [9]. The results for the signal process are presented without considering the possible interferences between the direct transition and the χ_{cJ} states, due to a lack of theoretical guidance. The distribution of the normal angle of the $\psi(3686)$ decay plane is characterized by the parameter $a = 0.53 \pm 0.68(\text{stat})^{+0.68}_{-0.27}(\text{syst})$, indicating a preference for a positive value. The J/ψ polarization parameter α was evaluated as $0.08 \pm 0.42(\text{stat})^{+0.07}_{-0.14}(\text{syst})$, demonstrating a competitive mixing of the longitudinal and transverse components. These results will help constrain the strength of the coupled-channel effect in future theoretical calculation. The reported branching fractions

$\mathcal{B}(\psi(3686) \to \gamma(\gamma J/\psi)_{\chi_{cJ}})$ are consistent with the world-average results [14]. The reported relative branching fractions of $\mathcal{B}_{\chi_{cJ}}$ are obtained with the world's best precision.

*Also at the Moscow Institute of Physics and Technology, Moscow 141700, Russia.

†On leave from the Bogolyubov Institute for Theoretical Physics, Kiev 03680, Ukraine.

‡Also at University of Piemonte Orientale and INFN, Turin 10125, Italy.

§Present address: INFN and University of Perugia, Perugia 06100, Italy.

‖Also at the PNPI, Gatchina 188300, Russia.

¶Present address: Nagoya University, Nagoya 464-8601, Japan.

[1] N. Brambilla *et al.*, Eur. Phys. J. C **71**, 1534 (2011).

[2] Y.-Q. Chen, N. Brambilla, Y. Jia, and A. Vairo, Int. J. Mod. Phys. A **24**, 295 (2009).

[3] E. J. Eichten, K. Lane, and C. Quigg, Phys. Rev. D **69**, 094019 (2004); X. Liu, Phys. Lett. B **680**, 137 (2009); T. Barnes, in *Proceedings of the XIII International Conference on Hadron Spectroscopy*, edited by V. Crede, P. Eugenio, and A. Ostrovidov, AIP Conf. Proc. No. 1257 (AIP, New York, 2010), p. 11.

[4] B. Q. Li and K. T. Chao, Phys. Rev. D **79**, 094004 (2009).

[5] Z.-G. He, X.-R. Lu, J. Soto, and Y. Zheng, Phys. Rev. D **83**, 054028 (2011).

[6] K. Pachucki, D. Leibfried, M. Weitz, A. Huber, W. König, and T. W. Hänsch, J. Phys. B **29**, 177 (1996); A. Quattropani and F. Bassani, Phys. Rev. Lett. **50**, 1258 (1983).

[7] J. Z. Bai *et al.* (BES Collaboration), Phys. Rev. D **70**, 012006 (2004); M. Ablikim *et al.* (BES Collaboration), *ibid.* **71**, 092002 (2005).

[8] N. E. Adam *et al.* (CLEO Collaboration), Phys. Rev. Lett. **94**, 232002 (2005).

[9] H. Mendez *et al.* (CLEO Collaboration), Phys. Rev. D **78**, 011102(R) (2008).

[10] M. Ablikim *et al.* (BESIII Collaboration), Nucl. Instrum. Methods Phys. Res., Sect. A **614**, 345 (2010).

[11] M. Ablikim *et al.* (BESIII Collaboration), Phys. Rev. D **81**, 052005 (2010).

[12] C. Zhang, Sci. China Ser. G **53**, 2084 (2010).

[13] S. Jadach, B. F. L. Ward, and Z. Was, Phys. Rev. D **63**, 113009 (2001).

[14] J. Beringer *et al.* (Particle Data Group), Phys. Rev. D **86**, 010001 (2012).

[15] R. G. Ping, Chinese Phys. C **32**, 599 (2008).

[16] J. C. Chen, G. S. Huang, X. R. Qi, D. H. Zhang, and Y. S. Zhu, Phys. Rev. D **62**, 034003 (2000).

[17] S. Agostinelli *et al.* (GEANT Collaboration), Nucl. Instrum. Methods Phys. Res., Sect. A **506**, 250 (2003); J. Allison *et al.*, IEEE Trans. Nucl. Sci. **53**, 270 (2006).

[18] G. Karl, S. Meshkov, and J. L. Rosner, Phys. Rev. D **13**, 1203 (1976); M. A. Doncheski, H. Grotch, and K. J. Sebastian, *ibid.* **42**, 2293 (1990).

[19] P. Artoisenet, J. P. Lansberg, and F. Maltoni, Phys. Lett. B **653**, 60 (2007).

[20] M. Ablikim *et al.* (BESIII Collaboration), Phys. Rev. Lett. **104**, 132002 (2010).